Novel Methods of Measuring Hydraulic Conductivity of Tree Root Systems and Interpretation Using AMAIZED[1]

A Maize-Root Dynamic Model for Water and Solute Transport

Melvin T. Tyree*, Shudong Yang, Pierre Cruiziat, and Bronwen Sinclair

Northeastern Forest Experiment Station, Burlington, Vermont 04502 (M.T.T.); Department of Botany, University of Vermont, Burlington, Vermont 05405 (S.Y.); and Institut National de la Recherche Agronomique, Laboratoire de Physiologie Integree de l'Arbre Fruitier, 63039 Clermont-Ferrand, France (P.C., B.S.)

Steady-state and dynamic methods were used to measure the conductivity to water flow in large woody root systems. The methods were destructive in that the root must be excised from the shoot but do not require removal of the root from the soil. The methods involve pushing water from the excised base of the root to the apex, causing flow in a direction opposite to that during normal transpiration. Sample data are given for two tropical (*Cecropia obtusifolia* and *Lacistema aggregatum*) and two temperate species (*Acer saccharum* and *Juglans regia* cv Lara). A hysteresis was observed in the relationship between applied pressure and resulting flow during dynamic measurements. A mathematical model (AMAIZED) was derived for the dynamics of solute and water flow in roots. The model was used to interpret results obtained from steady-state and dynamic measurements. AMAIZED is mathematically identical with the equations that describe Münch pressure flow of solute and water in the phloem of leaves. Results are discussed in terms of the predictions of AMAIZED, and suggestions for the improvement of methods are made.

Water and solute transport dynamics are documented best in extensive studies of maize roots (Frensch and Steudle, 1989; Azaizeh and Steudle, 1991). In this paper we show how a maize root model of solute and water transport can be generalized and used to interpret methods of measuring hydraulic conductivity of large root systems of woody plants.

Both root and shoot conductivities (K_r and K_s, respectively) to water transport are important parameters in the water relations of woody plants. These parameters are needed in models of the soil-plant-atmosphere continuum in order to predict the rate of water flow through whole plants and to predict the water potentials, Ψ, in various organs of plants. K_s is relatively easy to estimate (Tyree and Ewers, 1991; Tyree et al., 1993a, 1993b), but K_r and whole plant conductivity, K_w, are difficult to estimate on large woody plants. The usual method requires a measurement of (a) soil water potential, Ψ_{soil}, from predawn leaf water potential, Ψ_{lpd}; (b) midday leaf water potential, Ψ_{leaf}; and (c) midday evaporative flux density, E, which is usually estimated from stem water flow measurements divided by leaf area (Cermák et al., 1980; Bréda et al., 1993). Whole plant conductivity (for the liquid pathway), K_w, is calculated from $E/(\Psi_{lpd} - \Psi_{leaf})$. If an independent estimate of the Ψ at the base of the plant, Ψ_b, is obtained (e.g. from a bagged, nontranspiring leaf), then root conductivity can be calculated from $K_r = E/(\Psi_{lpd} - \Psi_b)$.

Measurements of K_w and K_r are usually subject to a number of sources of error. Stem flow measurements used to estimate E usually have a range of accuracy of 10 to 20%. Single-leaf values of E estimated with a porometer on large trees are more accurate, but a representative number of leaves in different parts of the crown must be measured to obtain an accurate average value. The error in sampling a representative number of leaves is unknown but could easily be >20%. Also, Ψ_{soil} is rarely measured at the root surface; it is equated to predawn leaf water potential, Ψ_{lpd}, and assumed to be unchanged at midday. In dry soils, K_w and K_r can be underestimated by a factor of 2 to 4 (Bréda et al., 1993) because during the day the Ψ at the root/soil interface can decrease below Ψ_{lpd} due to the low conductivity to water in dry soils. A more direct measurement of K_r would be desirable and necessary if we are to separate the effects of soil conductance from root conductivity.

Abbreviations: A_L, leaf area (m^2); C, solute concentrations (subscripts: i, in vessels; o, outside root) [osmol m^{-3}]; d, diameter of root [m]; D, diffusion coefficient of small solutes in water (m^2 s^{-1}); E, evaporative flux density from leaves (kg s^{-1} m^{-2}); F, mass flow rate (kg s^{-1}); J_{sol}, radial solute flux density in roots (osmol m^{-2} s^{-1}); J_s, radial solute flux density due to active transport (osmol m^{-2} s^{-1}); J_v, radial water flux density in roots (m s^{-1}); J_w, volume flux density of water in vessels of root (m^3 s^{-1} m^{-2}); K_r and K_s, whole root and shoot conductivities, respectively (kg s^{-1} MPa^{-1} m^{-2} [of leaves]); K_{st}, stem conductivity with leaves removed (kg s^{-1} m^{-2} MPa^{-1}); L, length of absorbing zone in root (m); L_P, radial conductivity to water flow in roots (m s^{-1} MPa^{-1}); L_x, axial conductance to water flow in roots (m^2 s^{-1} MPa^{-1}); P, pressure (MPa); P_s, radial solute permeability in roots (m s^{-1}); R, gas constant (MJ osmol^{-1} $^\circ K^{-1}$); v, axial velocity of sap in osmotic volume (= vessels?) of root; V_f, osmotic volume of absorbing zone of root as fraction of volume of root (= [cross-section of vessel lumina]/[root cross-section]?); σ, reflection coefficient; Ψ, water potential (MPa).

In this paper we explore novel methods of measuring K_r in situ in woody plants. The methods are destructive in that root systems must be excised from shoots, but the methods do not require removal of the roots from the soil. A dynamic model for solute and water flow in maize (*Zea mays* L.) roots is used to interpret our results and to suggest improved methods.

MATERIALS AND METHODS

Plant Material and Sites

Studies of *Cecropia obtusifolia* Ertol. (family Moraceae) and *Lacistema aggregatum* Berg (family Ulmaceae) were conducted in March 1992 (dry season) on Barro Colorado Island, Panama (9° 7.5' N, 79° 52' W). Irrigation with a sprinkler was applied for several days to thoroughly wet the soil. Studies of walnut (*Juglans regia* L. cv Lara) were conducted on saplings growing in 200-L pots containing a 1:1 mixture of garden clay soil and peat moss. Experiments on *Acer saccharum* Marsh. were conducted in the field at the Proctor Maple Research Center (Underhill Center, VT).

Experiments were conducted on 20- to 30-mm-diameter *Cecropia* roots excavated from near the base of a 5-m *Cecropia*. All other experiments were conducted on entire root stocks that were 25 to 45 mm in diameter. In all cases a water-tight reservoir was constructed around the base of a shoot near ground level (or around a *Cecropia* root). The reservoir was filled with water, and the root or root stock was cut under water. In the case of walnut, the shoot excised from the root stock was kept in water, and later the hydraulic conductivity of the shoot, K_s, was measured. Water-filled Tygon tubing was clamped over the root, root stock, or shoot and connected to a system for measuring flow versus pressure applied.

K_r Measurement

K_r was estimated by applying a positive pressure, P, and forcing distilled water into the base of the root (opposite to the normal direction of water flow during transpiration). The water flux, F (kg s^{-1}), was measured, and K_r was calculated from the slope of the plot of F versus P:

$$K_r = (1/A_L) \, \Delta F/\Delta P \qquad (1)$$

where A_L is the leaf area fed by the root. Division by A_L permitted comparison of absolute root conductance ($\Delta F/\Delta P$) to shoot conductance as is usually done in hydraulic architecture studies (Tyree and Ewers, 1991). The usual practice is to report root conductance per unit root surface area, but this makes sense only if two conditions are true, i.e. only if flow is approximately uniform over the root surface area and only if the main barrier to flow is located at the outer surface rather than some other surface, e.g. the Casparian band. Both conditions are doubtful in large root systems in which the contribution of old versus young roots to radial flow is uncertain. Division by root surface area makes comparisons of root conductance to shoot conductance more difficult. When A_L was not measured, then the absolute conductance was computed and will be referred to in this paper as A_LK_r. K_r was estimated from steady-state and dynamic-state measurements.

Steady-State Measurements of K_r

The base of the root was connected to water-filled tubing and supplied with water from a beaker that rested on a digital balance. A microcomputer was programmed to read the weight of the beaker at fixed intervals and to compute F. P was increased by raising the balance from 0 to 16 m above the root base (corresponding to a 0- to 0.16-MPa change in P). This was achieved by studying plants growing on a hillside and moving the balance up and down the hill. Steady state was assumed to be reached when F became constant (usually in 1–2 h).

Dynamic Measurements of K_r

Rapid measurements of K_r were performed on walnut roots in soil irrigated to field capacity.

Flow through large root systems in wet soil is probably rate limited by the radial conductivity to water, L_P (m s^{-1} MPa^{-1}), in the absorbing zone of roots. The driving force for radial flux density [J_v (m s^{-1})] is given by $\Delta P - \sigma RT\Delta C$, where ΔP is the pressure difference across the radius of the root, σ is the reflection coefficient, ΔC is the solute concentration difference across the radius, and R and T are the gas constant and absolute temperature, respectively. Therefore,

$$J_v = -L_P(\Delta P - \sigma RT\Delta C) \qquad (2)$$

During steady-state measurements of K_r, it is possible that ΔC increases with increasing F because solutes are pushed backward toward the root tips and concentrated by reverse osmosis. Therefore, an attempt was made to measure F in a time brief enough to minimize change in ΔC.

The base of the root was connected to a high-pressure flowmeter described in detail elsewhere (Tyree et al., 1993b). Briefly, the flowmeter consisted of a water reservoir that could be pressurized with compressed air from a pressure regulator. Water flow rate from the reservoir to the base of the excised root was computed from the measured pressure decrease across a capillary tube interposed between the reservoir and root. The capillary tube was 0.5 mm i.d. and 0.12 m long. The flowmeter was calibrated and found to have a flow of 1.39×10^{-8} kg s^{-1} Pa^{-1} pressure decrease across the capillary tube. The reproducibility of pressure measurement was ±10 Pa (±1 mm of water level, measured with water manometers), giving a flow accuracy of ±1.4 × 10^{-7} kg s^{-1}. The response time of the flowmeter was 53 s to reach 90% of the steady-state reading.

The flowmeter permitted adjustments of pressure at a rate of 1.6 kPa s^{-1} and accurate flow measurements within 100 s of the pressure change. Therefore, P could be adjusted and F measured within 3 min.

K_{st} and K_s

The whole walnut shoot, excised from the root stock, was connected to the flowmeter and pressurized at $P = 0.2$ MPa for 2 h. During this time the leaf air spaces filled with water and water began dripping from the stomates of leaves. After a stable flow was achieved, the whole shoot conductivity, K_s, was computed from $K_s = F/(PA_L)$. The leaves were then

removed, causing F to increase and stabilize within 2 min. Stem conductivity was computed from $K_{st} = F'/(PA_L)$, where F' is the flow with leaves removed.

RESULTS

Two examples of steady-state measurements on roots over a small pressure range are shown in Figure 1, A and B, for *C. obtusifolia* and *L. aggregatum*. Data for *L. aggregatum* and *A. saccharum* measured over higher pressure ranges are shown in Figure 1, C and D. F was a linear function of P, although some hysteresis was found. Values of absolute root conductance are given in Figure 1, A through D.

There was a reproducible hysteresis in walnut roots, and the shape of the hysteresis depended on the timing of experiments. Shoots were excised by 10:00 AM; therefore, the trees had transpired for 2 to 3 h. When F measurements on roots were made within 15 to 20 min of excision, a narrow hysteresis was observed with a high average slope (open circles in Fig. 2A). Flows were higher while P was increased in three steps from 0.01 to 0.21 MPa. F decreased along a lower path when P was decreased in four steps to 0.01 MPa. This behavior was observed in three of three trees in which measurements were started within 15 to 30 min of excising the shoots. After the trees were allowed to stand and exude sap freely at a pressure of 0.01 MPa for >1 h, a different hysteresis was observed. The first loop was open ended (data not shown), but after the first cycle of pressure changes the same hysteresis curve was observed up to four times on
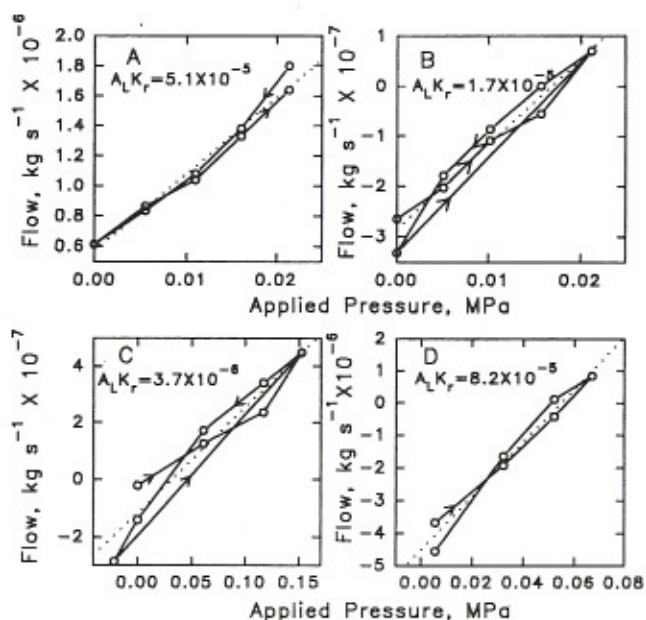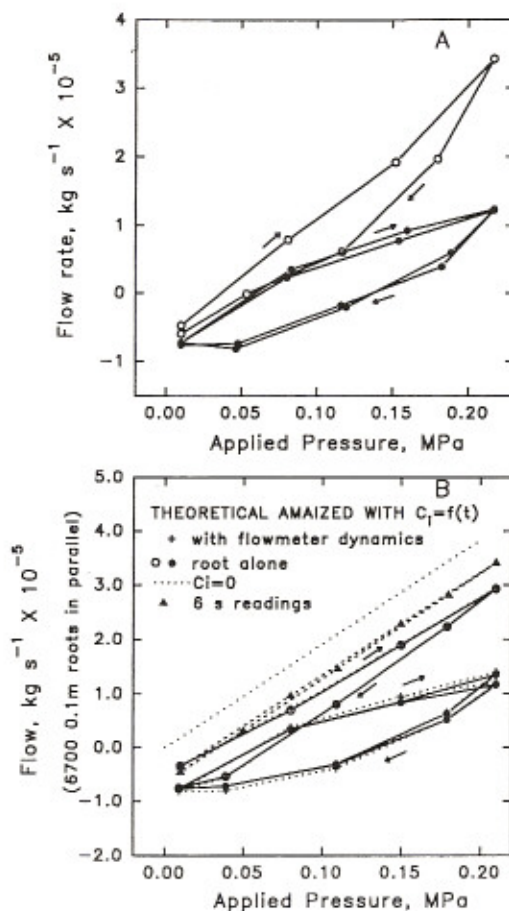

Figure 2. A, Dynamic measurement of flow versus applied pressure on *J. regia*. Pressures were changed and flows measured in 2.5 to 3 min per point. The direction of pressure change is indicated by arrows. Open circles, Values measured 20 min after excising the shoot; filled circles, values measured 2 h after excising the shoot. B, Theoretical predictions from AMAIZED, the model for the dynamics of solute and water transport in roots. Values used in the model were those given in Table II for walnut. Dotted line, Predictions when solute concentration in vessels = 0; dashed line with triangles, predictions for measurements taking 6 s per reading; solid lines with open circles, predictions of AMAIZED 20 min after excising the shoot; solid lines with filled circles, predictions of AMAIZED 1.5 h after excising the shoot; dotted lines with +'s, predictions of AMAIZED when the response time of both the root and flowmeter are taken into account. Because +'s are close to open and filled circles, we can conclude that the hysteresis was due to the dynamics of the root rather than the response time of the flowmeter.

Figure 1. Steady-state measurements of root conductance. Flow rate, F, is plotted versus applied pressure at base of root system. The root conductance, $A_L K_r$, is the slope of the best fit line (dotted line in A–D). The sequence of pressure change is indicated by arrows. A and B, Low-pressure measurements on *C. obtusifolia* and *L. aggregatum* (plant 1), respectively. C and D, High-pressure measurements on *L. aggregatum* (plant 2) and *A. saccharum*, respectively.

subsequent pressure cycles. Figure 2A (closed circles) shows the second and third cycles. Similar data were obtained from five of five trees.

Values of K_r, K_s, and K_{st} for walnut are shown in Table I. K_r values were based on linear regressions of the entire hysteresis loop. The water relations of similar sized walnut trees growing under similar conditions were documented previously in trees irrigated daily to field capacity (Tyree et al., 1993a). Ψ_{leaf} and Ψ_{st} were measured by determining the

Table I. *Root and shoot conductivities and water relations of walnut trees measured at midday*

Time refers to the time elapsed after the shoot was excised prior to measurement of K_r. $K_r(3c)$ and $K_r(3d)$ were computed values from Equations 3c and 3d, respectively.

	Individual Root Values		
Sample	A_L	K_r	Time
	m^2	$kg\ s^{-1}\ m^{-2}\ MPa^{-1}$	h
Root 1	3.07	3.25×10^{-5}	2.0
Root 2	2.87	3.29×10^{-5}	2.0
Root 3	4.11	9.76×10^{-5}	0.4
Root 4	3.67	5.15×10^{-5}	0.5
Root 5	2.68	16.6×10^{-5}	0.3

		Mean Shoot Values and Computed K_r					
E	Ψ_{leaf}	Ψ_{stem}	K_s	K_s	$K_r(3c)$	$K_r(3d)$
$kg\ s^{-1}\ m^{-2}$	MPa			$kg\ s^{-1}\ m^{-2}\ MPa^{-1}$		
Mean 6×10^{-5a}	-0.7^a	-0.5^a	14×10^{-5}	48×10^{-5}	16×10^{-5}	22×10^{-5}
SD 1×10^{-5}	0.1	0.1	3×10^{-5}	6×10^{-5}	—	—

[a] Values from Tyree et al. (1993b). K_s and K_{st} values are pooled values from two shoots measured in this study and five shoots measured by Tyree et al. (1993b).

balance pressure with a pressure chamber on exposed and bagged leaves, respectively. The average evaporative flux density from leaves, E, was also estimated from measurements using a custom-built stem flow gauge (Valancogne and Nasr, 1989a, 1989b). From these data (Table I) an independent estimate of K_r could be computed as follows. The Ψ at the base of the root stock, Ψ_b, was estimated from

$$\Psi_b = \Psi_{leaf} + E/K_s \qquad (3a)$$

or

$$\Psi_b = \Psi_{st} + E/K_{st} \qquad (3b)$$

Then, assuming that $\Psi_{soil} = 0$ in soil watered to field capacity, K'_r was calculated from E/Ψ_b according to:

$$K'_r = -E/(\Psi_{leaf} + E/K_s) \qquad (3c)$$

or

$$K'_r = -E/(\Psi_{st} + E/K_{st}) \qquad (3d)$$

The values of K_r measured with the high-pressure flowmeter soon after excising the shoots were close to the independent estimates but were underestimated by a factor of 3 to 5 when measured >2 h after the shoots had been excised. It could be argued that the values of K'_r computed from Equation 3d were more accurate than those from Equation 3c because of the large decrease in Ψ within leaf blades, which we estimate to be 0.3 MPa when $E = 6 \times 10^{-5}$ kg s^{-1} m^{-2}. When the leaf is excised and placed in the pressure chamber, the value of Ψ_{leaf} measured will be somewhere between that at the base of the leaf and that at the evaporating surface. The value used in Equation 3c should be the latter, and if it had been -0.8 MPa, then the values computed by Equations 3c and 3d would have been equal.

DISCUSSION

The hysteresis of flow (F) versus applied pressure (P) observed in the walnut data might be due to the dynamics

of solute concentration changes, C_i, in walnut roots. This follows because F is determined by the difference in Ψ ($\Delta\Psi$) across the root, i.e. by differences in pressure and solute potential ($\Delta P - RT\Delta C$). Thus, if C_i changes while P changes, there may not be a linear relationship between F and P. It also seems likely that K_r was underestimated when hysteresis occurred (Table I). Perhaps even the steady-state values of $A_L K_r$ (Fig. 1) were underestimated even though F was approximately proportional to P. This could happen if C_i increased in proportion to the rate of flow, causing $\Delta\Psi$ to increase less than ΔP, but we have no independent measurements of $A_L K_r$ to check against. A model to describe the dynamics of changes in C_i caused by water flow into and out of roots was derived and used to interpret our data. The concept of measuring K_r by pushing fluid backward down a root as reported in this paper is not new, and it has been suggested that the method might cause errors. The model will allow us to evaluate possible sources of error.

AMAIZED: Model and Theory

The equations that determine the rate of water and solute flow in maize roots are well known (Anderson et al., 1970; Fiscus and Kramer, 1975; Azaizeh and Steudle, 1991); therefore, a model was derived for how C_i will change with time and distance in roots during measurements such as those reported in this study. The root (Fig. 3) was divided into a tip, where negligible flows of solute and water occur, a source zone, where substantial radial and axial flux densities of solute and water occur, and a transport zone, where only axial flow occurs. The model does not restrict the age or diameter or anatomical state of the source zone, i.e. it could include suberized roots or roots with secondary growth. The source zone is defined only as the region where substantially larger radial fluxes occur than in the transport zone and the tip. The source zone could include the entire root system, in which case the transport zone would be confined to the shoot. The source zone is divided into n elements of length ΔX and diameter d ($n = 100$–300 elements). Radial transport
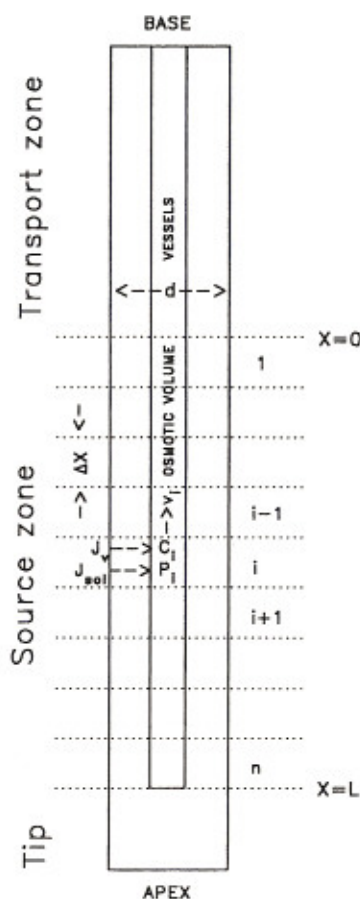
Figure 3. Diagram of a root divided into a tip, a source zone, and a transport zone. This figure shows quantities used in AMAIZED and how the source zone was divided into segments for computational analysis. The source versus transport zones are defined as regions with substantial radial fluxes of water and solute versus negligible radial fluxes, respectively. The model does not specify the developmental stage at which transition occurs. For simplicity, the model provides for a discontinuous transition between zones, whereas in real roots the transition may occur over many millimeters distance.

occurs from the outside of the root to an osmotic space tentatively identified with the volume of all vessel lumina in the source zone; let V_f be the osmotic volume as a fraction of root volume. We assume that P and C rapidly equilibrate within any one element in the source and transport zones.

The equations that govern radial flux densities in any element of this system are:

$$J_v = -L_P [P_i - \sigma RT(C_i - C_o)] \tag{2}$$

where C_o is the concentration of solute outside the root, and

$$J_{sol} = J_s - P_s (C_i - C_o) \tag{4}$$

where J_{sol} is the net solute flux density, J_s is the active influx of solute due to root metabolism, and P_s is the solute permeability.

The equations that govern axial flux density in any element are:

$$J_D = -D \, \Delta C_i / \Delta X \tag{5}$$

where J_D is the axial diffusional solute flux density from Fick's first law, D is the coefficient of diffusion, and ΔC_i is the difference in C between adjacent elements, and

$$J_w = -L_x \, \Delta P_i / \Delta X \tag{6}$$

where J_w is the axial volume flux density (m s^{-1}) down the vessels, L_x is the axial conductance (m^2 s^{-1} MPa^{-1}), and ΔP_i is the pressure decrease across the ith element.

These equations were solved using standard iterative computational techniques. The details of the derivation are omitted here because the equations and model system (Fig. 3) are mathematically identical with the equations that govern Münch pressure flow in the loading zone of phloem in leaves; equations for this system have been thoroughly developed in the past (Christy and Ferrier, 1973; Tyree et al., 1974; Goeschl et al., 1976). The core of the working program called AMAIZED is given in "Appendix" for anyone wishing to use the model or to examine the equations in detail. Similar sets of equations have been used to obtain steady-state solutions of solute and water transport in roots (Anderson et al., 1970; Fiscus and Kramer, 1975). However, non-steady-state solutions have not been published.

Although the equations are not derived here, it will be useful to examine the iterative equation for the rate of change of C in the ith element to see what factors cause changes in C. The rate of change of C ($\Delta C/\Delta t$) will be determined by the sum of changes caused by radial solute fluxes ($\Delta C_r/\Delta t$), by axial diffusion ($\Delta C_D/\Delta t$), and by axial mass flow ($\Delta C_w/\Delta t$):

$$\frac{\Delta C}{\Delta t} = \frac{\Delta C_r}{\Delta t} + \frac{\Delta C_D}{\Delta t} + \frac{\Delta C_w}{\Delta t} \tag{7a}$$

$$\frac{\Delta C}{\Delta t} = \frac{4}{dV_f}(J_s - P_sC_i) + \frac{D}{\Delta X}(C_{i-1} + C_{i+1} - 2C_i) + \frac{4L_P}{dV_f}f(C, J_w) \tag{7b}$$

where $f(C, J_w)$ represents a complex summation of terms containing the product of C times J_w in all elements of the root; CJ_w gives the axial mass flux density of solutes in any element. J_w is determined by P, $\sigma RT\Delta C$, L_P, and L_x. The middle term for diffusion in Equation 7b is negligible under most circumstances. Therefore, the dynamics of changes in C with time and distance were determined primarily by ($4/dV_f$), L_P, and ($J_s - P_sC_i$). Most of the dynamics influencing the measurements in this paper were contained in the last term and were due to mass displacement of solute and the large concentration changes inside the root caused by reverse osmosis when solution was forced back into the root.

The parameters used in the model were those in Table II. Maize parameters were used because a complete set of accurate data could not be found for any other species. One assumption made was that the resistance to water flow along the axis of roots is less than the radial resistance. In AMAIZED this was achieved by arbitrarily setting $L_x = 5\pi dL^2L_P$. This was within the range of values reported for some roots (Nobel and Sanderson, 1984; Frensch and Steudle, 1989; North et al., 1992).

Table II. *Transport parameters used in AMAIZED*

Maize values taken from Azaizeh and Steudle (1991) except as indicated. Walnut values are those used to fit data in Figure 2B.

Parameter (units)	Maize Values	Walnut Values
L_P (m s^{-1} MPa^{-1})	2×10^{-7}	2.2×10^{-7}
P_s (m s^{-1})	3×10^{-9}	2.3×10^{-9}
σ	0.7	0.7
J_s (mol m^{-2} s^{-1})	1.76×10^{-7a}	1.16×10^{-7}
L (m) (but unimportant)	0.1	0.1
d (mm)	1.0	0.76 (0.10)^c
L_x (m^4 s^{-1} MPa^{-1})	$5\pi dL^2 L_P$	$5\pi dL^2 L_P$
V_f	0.03^b	0.021 (0.003)^c

^{a} J_s computed from steady-state root pressure with zero flow, i.e. $J_v = L_P (\Delta P - \sigma RT\Delta C) = 0$ and $J_{sol} = J_s - P_s\Delta C = 0$, so $J_s = P_s \Delta P/\sigma RT$. ^{b} Assumed to be the ratio of volume of vessel lumina/volume of root = cross-section of vessels/cross-section of root. Vessel dimension and numbers were taken from figure 3 of Peterson et al. (1993). ^{c} Values for roots with mature metaxylem measured on walnut trees in this study; values given as mean (SE), $n = 9$.

Another simplifying assumption was that the change in C_o was less than the change in C_i; therefore, C_o can be set to a small constant value such as the low concentration of solutes in the soil solution, i.e. 0.01 to 0.2 osmol m^{-3} (Nobel, 1991, p 156). We have selected a combined solute concentration value of $C_o = 5$ osmol m^{-3}, which was close to the measured value in the irrigation water used in this study (4 osmol m^{-3}). This value was still high enough to permit J_s, which was governed by Michaelis-Menten type kinetics, to be near a constant maximum value. C_o will change because of convective and diffusive fluxes of solute at the root surface. Preliminary calculations of radial diffusion in soils revealed that, when there was net solute uptake ($J_{sol} > 0$), C_o decreased a few osmol m^{-3} near the root surface, and, when J_{sol} was <0, C_o increased a similar amount. Preliminary calculations of AMAIZED revealed that changes in C_i were of the order of 10^2 osmol m^{-3}. Therefore, it was valid to treat C_o as a constant.

Predictions and Properties of AMAIZED

We examined predictions of AMAIZED under two classes of conditions: (a) steady-state flow and (b) dynamic flow in which P at the base of the root was either a stepwise function of time or a sawtooth function of time.

Steady-State Solutions

The steady-state solutions of AMAIZED allowed us to determine whether the root conductance values ($A_L K_r$) in Figure 1 were correct. Figure 4 shows a steady-state solution of AMAIZED. The solid line with closed circles (Fig. 4A) represents F versus P for the case for which C_i and J_s were both zero. The slope of this line gave $A_L K_r$ and was the value resulting from the combined influence of radial and axial hydraulic conductivities, L_P and L_x, respectively. The dotted line connecting open circles was the predicted F versus P over the region for which $F < 0$, i.e. the normal direction of water transport in roots when P is negative because of transpiration. As P grew more negative F approached the solid line asymp-
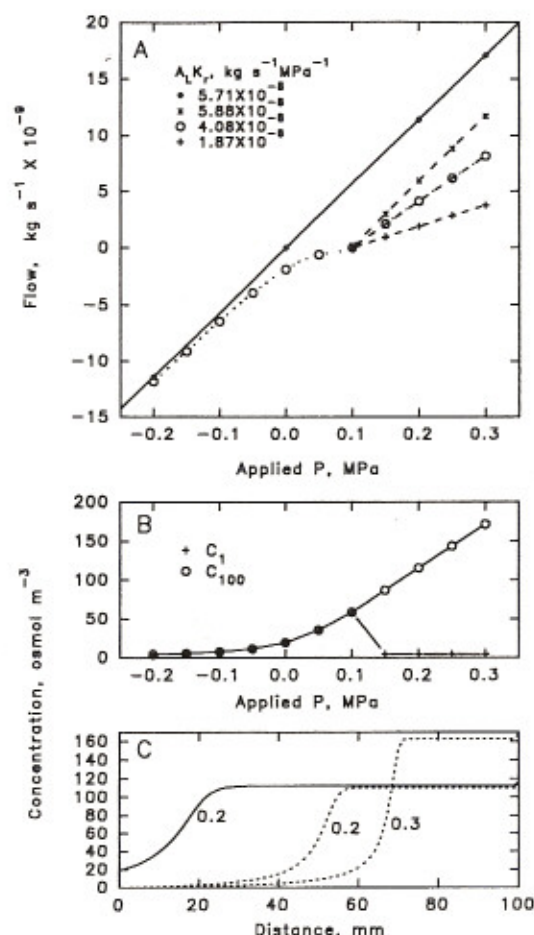

Figure 4. Steady-state predictions of AMAIZED; parameters used were those measured for maize roots (Table II). A, Flow versus applied pressure; negative flow indicates the normal direction of flow during transpiration, whereas positive flow is for flow from the base of the root toward the apex when $P > 0.1$ MPa. Solid line and filled circles, for root with no solutes in the xylem vessels and, therefore, $J_s = 0$. When flow is in the normal direction ($F < 0$ and $P < 0.1$), the concentration of solutes in vessels is determined by the dynamics of solute and water flow (open circles with dotted line). When flow is opposite to normal ($F > 0$ and $P > 0.1$), the trend of the curve depends on the concentration of solutes pushed down the root axis; trends shown are for the following concentrations (osmol m^{-3}) pushed into the root at $x = 0$ in Figure 3: 20 (+), 4.33 (open circles), 0 (x). Slopes for curves ($=A_L K_r$) are given. B, Concentration at the base (C_1) and at the apex (C_{100}) of the source zone versus applied pressure. For flow from the base into the root the perfusion concentration was held at 4.33 osmol m^{-3}. C, Predictions of AMAIZED for concentration profiles in the source zone of roots during steady-state perfusion ($F > 0$). Solid line is for source concentration = 20 osmol m^{-3} and applied pressure of 0.2 MPa. The dashed lines are for source concentration of 0 and applied pressures as indicated by numbers to the right of the dashed lines.

totically. The asymptotic approach to the solid line occurred because C_i approached 0 as P grew negative (Fig. 4B). In our experiments F was usually >0; therefore, the curve predicted by AMAIZED depended on the concentration of sap entering at element 1 ($C_i[x = 0]$, Fig. 3). If $C_i[x = 0] = 0$, then the curve followed the path indicated by X's in Figure 4A. It is unlikely that $C_i[x = 0]$ would ever equal zero in an experimental situation. Even if distilled water were perfused into a root system, it must pass through a long transport zone to reach the source zone. The solute concentrations must be buffered toward the average daily concentration experienced by the cells in the transport zone, i.e. C should be increased if the current value were less than the daily average value and should be decreased if the current value were more than the daily average value.

What is the likely daily average concentration in the source zone? AMAIZED predicted that C_i was almost constant along the axis of the source zone when $F < 0$ (see Fig. 4B for values of $P < 0.1$), and this was in accord with predictions of source concentrations in Münch pressure flow models (Tyree et al., 1974). Thus, C_i at element 1 will be given by:

$$C_i = J_{sol}/J_v \qquad (8)$$

Putting Equations 2 and 4 into Equation 8 yields the standard quadratic solution of

$$C_i = [-b + (b^2 - 4ac)^{0.5}]/2a \qquad (9a)$$

where

$$a = L_P \sigma RT \qquad (9b)$$

$$b = [P_s - L_P(P + \sigma RTC_o)] \qquad (9c)$$

and

$$c = -J_s - P_sC_o \qquad (9c)$$

During much of the day P might be -0.4 MPa and at night P might be 0 MPa. Calculated values of C_i equaled 2.3 and 21.8 osmol m^{-3} for $P = -0.4$ and 0 MPa, respectively, when the maize parameters in Table II were used. When the flow direction was opposite to normal ($F > 0$), the predicted relationship of F versus P depended on the concentration of solutes pushed down the root axis (see open circles and pluses in Fig. 4A).

AMAIZED predicted that the slope obtained for $F > 0$ was slightly more than the theoretical (5.88×10^{-8} versus 5.71×10^{-8} kg s^{-1} MPa^{-1}) when $C_i[x = 0] = 0$. This surprising result was a consequence of the change in profiles of C_i versus distance in the source zone as P increased (Fig. 4C). At $P = 0.2$, C_i was nearly zero in the basal half of the source zone, and in the apical half C_i was high enough to bring J_v nearly to zero. Therefore, at $P = 0.2$, radial water flux occurred out of the root only in the upper half. But at $P = 0.3$ the zone with high C_i was pushed down to the apical one-third of the root, and radial water flow occurred in the upper two-thirds. The net result of the changes in the concentration profiles was that AMAIZED predicted that the measured $A_L K_r$ would be nearly the real value if C_i in the transport zone could be reduced to zero during a long period of perfusion.

In Figure 5 are plotted profiles of C_i, P_i, J_v, and J_{sol} versus distance from the base of the source zone as predicted by AMAIZED when the perfusion $C_i[x = 0]$ was 1 osmol m^{-3} and $P = 0.2$ MPa at the base of the source zone. In the basal half of the root C_i was low, J_{sol} was nearly J_s, and J_v was large and <0 (indicating outward flow, which would be needed if $F > 0$). In the apical half of the root, C_i was high, J_{sol} was nearly equal to $-J_s$, and J_v had decreased nearly to zero.

The steady-state solutions allow us to make some useful suggestions for how to improve the measurement protocol for steady-state determination of K_r. First, measurements of F should not be made in the region where there is exudation ($F < 0$) because the slope of F versus P will be too small (see Fig. 4A for P from 0–0.1 MPa). Second, measurements of F should not be made in the region where F changes from negative to positive values because the slope in this region underestimates the root conductance and because there could be a large change in slope depending on $C_i[x = 0]$ when $F > 0$. Third, because of the above considerations, the values of $A_L K_r$ in Figure 1 were probably underestimated. Fourth, measurements of F should be made on roots preperfused with distilled water for a few hours to reduce C_i at the base of the source zone. Best results will be achieved if the roots are perfused at 0.4 MPa, and then steady-state readings are taken from 0.4 to 0.2 MPa. Simulations of AMAIZED indicate that, if F is recorded after 3 h of perfusion and values are then taken at 0.3 and 0.2 MPa 1 h after each pressure change, then better estimates of root conductance will result, depending on C_i. K_r will be 0.96 of the correct value if C_i has decreased to 1 and will be 0.9 of the correct value if C_i is 2. However,
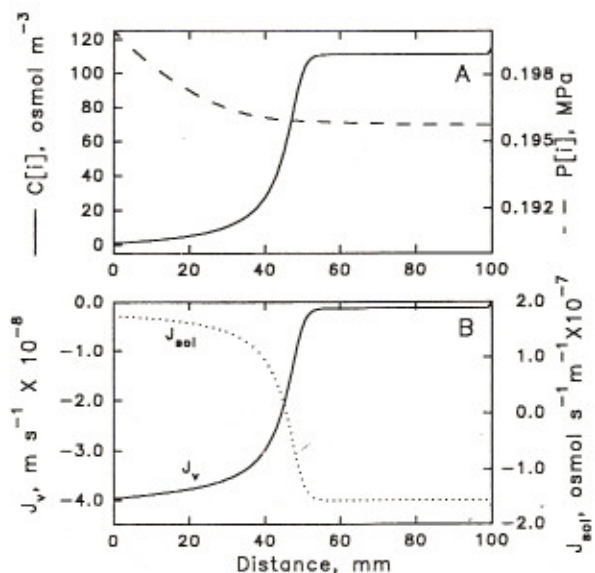

Figure 5. Steady-state predictions of AMAIZED; parameters used were those reported for maize roots (Table II). Distance on the x axis is the distance from the base of the source zone measured toward the apex. A, Steady-state profiles of concentration (C_i) and pressure (P_i) in vessels when C and P at the base of the source zone are 0 and 0.2, respectively. B, Profiles of radial solute flux density (J_{sol}) and of radial water flux density (J_v) under the conditions specified for A.

if tree roots have lower solute permeability (P_s) than maize roots or if preperfusion does not lower C_i enough, then preperfusion will not work, and A_LK_r will still be underestimated.

Dynamic Solutions

Our results indicated that K_r was underestimated when it was measured dynamically in walnut roots. Perhaps this was due to changes in C_i. The size of the error should depend on the time elapsed between a change in P and the measurement of F. After a long time, F and C_i will reach steady-state values (Figs. 4 and 5). In contrast, if measurements could be made fast enough so that there is little displacement of solution and thus little change in C_i, then the correct value of K_r should be obtained. At intermediate times, F and C_i will be in transition between initial and steady-state values, but it is not clear how much and in what direction this affects the estimate of K_r. Therefore, the AMAIZED model was used to predict the relationship between F and P for different rates of change of P.

The dynamics of water flow in a large root system should depend on both the dynamics of P versus time (t) and C_i versus t at the junction between the source and transport zones. This case will be examined below in the final walnut root model.

To learn how the source zone dynamics depend on P versus time alone, we examined the response of AMAIZED to a sawtooth change in P. The AMAIZED program given in "Appendix" was that used for a sine function loading of P (data not shown), but minor changes to the source code will allow the interested reader to study other kinds of dynamics, including steady-state dynamics. Below are some examples of computations of root dynamics in which the source concentration was equal to that reached by a root allowed to exude sap for several hours, i.e. C_i at the base of the source zone = 21.8 osmol m^{-3}.

When P versus t follows a sawtooth function as in Figure 6A, the resulting F also follows a distorted sawtooth function with a phase lag (Fig. 6B). The phase lag and distortion were more clearly seen when F was plotted versus P (Fig. 6C). AMAIZED predicted an open-ended cycle, followed by subsequent repeated hysteresis loops. The simulated data were qualitatively very similar to the actual data from walnut roots allowed to exude for >1 h prior to measurement, i.e. the first cycle in walnut was open ended with F higher at any given P than in subsequent cycles (data not shown).

Another important prediction of AMAIZED was that the dynamics of long- and short, absorbing zones were identical. Figure 6C shows the dynamics of four roots, each 25 mm long, working in parallel (+'s); F versus P for four short roots with a combined length of 0.1 m equaled the dynamics of one 0.1-m root (circles). This was a very important observation because it showed that a model of a single root can be extrapolated to describe a large complex root system. Thus, we can model very large root systems consisting of N roots in parallel using AMAIZED, provided (a) the main resistance to water flow resides in the source zone and (b) we interpret the other parameters used in Table II as being the arithmetic mean values of all N roots in parallel.
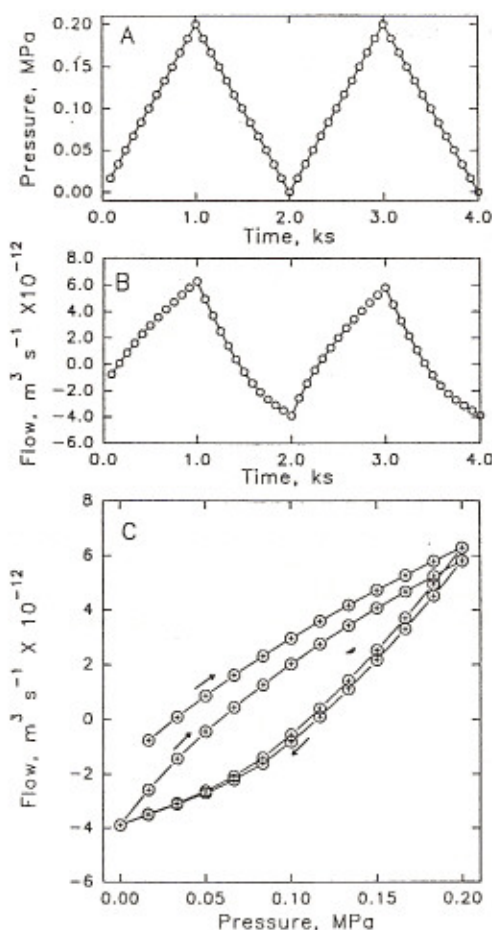

Figure 6. Non-steady-state (dynamic) predictions of AMAIZED; parameters used were those reported for maize roots (Table II). A, A sawtooth profile of applied pressure versus time. B, A distorted sawtooth profile of computed flow versus time as predicted by AMAIZED. C, A plot of flow versus applied pressure from A and B. Open circles, Prediction of AMAIZED for a single 0.1-m-long root. +, Prediction of AMAIZED for four roots each 25 mm long. After the first cycle of applied pressure versus time, the hysteresis loop repeats itself for the second and subsequent cycles.

Figure 7 shows the dynamic response of AMAIZED to changes in period of P versus t (= 1/frequency). Only the second cycle of F versus P is plotted. The slope of the curve marked $C_i = 0$ gave the correct value of A_LK_r for a maize root. When P was cycled with a period of 20 s, the curve of F versus P was displaced down on the plot, but the correct value of A_LK_r was obtained from the slope. The downward displacement of the curve was due to the nonzero value of C_i causing exudation ($F < 0$) at the lower values of applied P. When a 200-s cycle was used, the second cycle was open ended, but it still gave approximately the correct slope. When the period of the cycle was increased to 2,000 and 20,000 s, a hysteresis loop was formed by the second cycle, and the slope of the linear regression of the loop deviated progressively from the correct value of A_LK_r.

Figure 7 confirmed our hypothesis that rapid dynamic measurements of F versus P can yield the correct value for
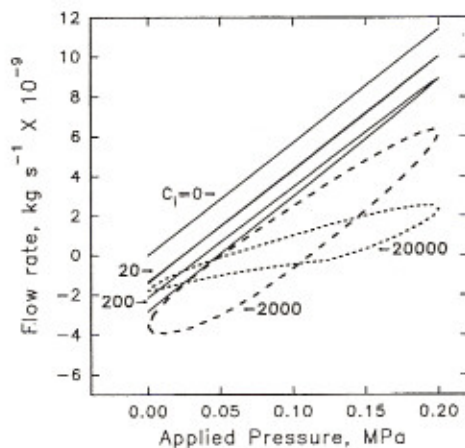
Figure 7. This figure is similar to Figure 6C but shows how the hysteresis of flow versus applied pressure changes with the period of applied pressure. The period is given next to each curve, in seconds. The upper line marked $C_i = 0$ is for the case when no solutes were present in the xylem; therefore, flow versus pressure will be independent of the period of the measurement.

root conductivity and that slower dynamic measurements will yield a hysteresis loop as in Figure 2A and that the slope of the entire hysteresis loop will underestimate A_LK_r. Rapid measurements of root conductivity would require an improved flowmeter with a response time of <1 s, i.e. about 100 times faster than the flowmeter used on walnut roots.

A sensitivity analysis of AMAIZED was conducted to determine how the hysteresis was affected by changes in the constants in Table II. The hysteresis curves were most affected by changes in $4L_P/dV_f$, which was the coefficient of the third term of Equation 7b. This was because rapid changes in C_i were caused mostly by the rate of axial flow in the source zone (the higher the L_P the higher was the axial flow) and by the volume of the osmotic zone, which was proportional to V_f (smaller V_f produces more rapid changes in C_i). The second most important combination of parameters was $(J_s - P_sC_i)$. This term measured the net radial solute flux density, and it determined (together with dV_t) how much time must elapse until a repeated hysteresis loop formed. The least important term was the diffusional term $\Delta C_D/\Delta t$ in Equation 7b, because the rate of change in C_i caused by diffusion was small in the space-time scale modeled by AMAIZED.

Walnut Root Model [Stepwise Changes in P with $C_i = f(t)$ at $x = 0$]

The dynamics of a large root system will be more complicated than that modeled in Figures 6 and 7 because of the influence of the transport zone (Fig. 3). For example, if the shoot of a walnut tree is excised in midmorning after a few hours of transpiration, then C_i in the transport zone will be uniformly low for a long distance basipetal to the source zone. But if the root system is allowed to exude freely (i.e. no pressure is applied at the base of the root stock), then the concentration of the exudate will gradually increase. The first

exudate to enter the transport zone will have traveled the farthest, and the last to enter will be the first to return to the root when the root stock is pressurized. The AMAIZED model was adapted to take into account the time sequence of pressure changes during the walnut experiments. It also accounted for the kinetics of C versus t and distance in the transport zone. This amounts to having a time-dependent $C_i(t, $ at $x = 0)$. The model was then allowed to simulate the exact timing of the experiments shown in Figure 2.

The following sequence of pressure changes was modeled:

1. A 0.5-h transpiration period with P_i set to -0.4 MPa. AMAIZED predicted that C_i decreased to a steady-state value of 1.55 osmol m^{-3} within a few minutes and that sap displacement exceeded 2 m, completely filling the transport zone with dilute sap.

2. A 20-min period with $P = 0.01$ MPa. This simulated the time lapse between cutting off the shoot and the time of the first measurement of F. During this time AMAIZED predicted a gradual increase in C_i and some exudation, but steady state was not reached.

3. One measurement sequence as in Figure 2A was simulated, i.e. P was increased in three steps from 0.01 to 0.21 MPa and then decreased to 0.01 MPa in four steps.

4. A 1-h period with $P = 0.01$ MPa was simulated. During this time AMAIZED predicted the approach of a near steady-state exudation rate and a total sap displacement in excess of 0.3 m into the transport zone. Therefore, this zone was now filled with sap at 22.5 osmol m^{-3}.

5. Three more cycles of measuring F versus P. The simulation results are shown in Figure 2B. F was scaled to allow for 670 m of roots in parallel (e.g. 6700 roots each 0.1 m long). The walnut root parameters needed to fit our experimental data are shown in Table II. We also demonstrated (by simulation of AMAIZED) that it may be possible to get the correct value of A_LK_r if measurements are made with 6 s allowed per pressure step (+'s in Fig. 2B).

AMAIZED can be verified only by comparing the predicted values of F versus P with those actually measured, and the predictive value of AMAIZED was very good (Fig. 2, A versus B). But the internal calculations provided some explanation as to why the hysteresis was observed in the walnut data. Figure 8C shows plots of the predicted values of $C_i(t, x = 0)$ and the total linear displacement of the liquid column from the source zone to the transport zone during the simulated measurement of F versus P. AMAIZED predicted rapid changes in C_i from 18 to 80 osmol m^{-3} and a linear displacement of fluid equal to the length of the root (100 mm). The implication for our walnut root experiments was that the entire volume of solution in the source zone of the roots was displaced by solution forced axially into the root by the applied pressure. The increase in concentration resulted from reverse osmosis as water (but not solute) was forced out of the root system.

Figure 8, A and B, also show "snapshot" images of profiles of C_i and resulting J_v, versus distance in the source zone. After the first pressure step (P1, from 0.01–0.08 MPa) the C_i profile was almost fully developed, and it did not change much by the last pressure step (P2, from 0.14–0.21 MPa). J_v increased with increasing P, however. At the end of the last
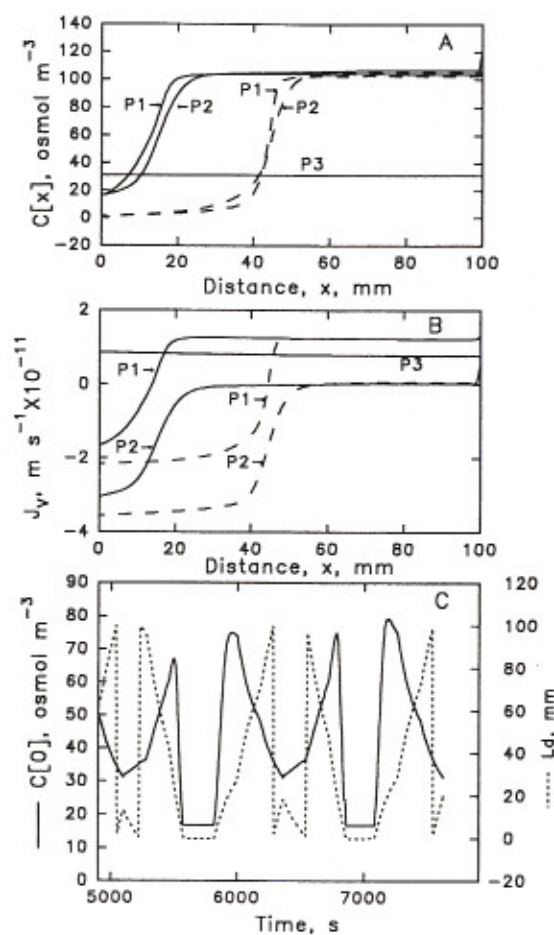
Figure 8. Dynamic profiles of selected parameters during non-steady-state flow in *J. regia* (walnut) roots. Profiles are those predicted by AMAIZED using the walnut parameters shown in Table II. Distance on the x axis of A and B is the distance from the base of the source zone measured toward the apex. A, Concentration profiles 20 min after excising the shoot (dashed lines) and 1.5 h after excising the shoot (solid lines). *P1* is the profile 3 min after increasing the applied pressure from 0.01 to 0.08 MPa, and *P2* is the profile 3 min after increasing the applied pressure from 0.14 to 0.21 MPa. *P3* is the profile 3 min after decreasing the pressure from 0.06 to 0.01 MPa. B, Similar to A except it shows profiles of radial water flux density (J_v). C, Solid line, Concentration at the base of the source zone (C[0]) versus time during the simulation of flow dynamics in walnut. Dashed line, Cumulative linear displacement of water column in vessels computed at base of source zone. Note that the total linear displacement is equal to the total length of the root, i.e. there is a complete solution replacement during the course of the simulated measurements. See text for more details.

step (*P3*, when *P* decreased from 0.06–0.01 MPa) the computed concentration profiles were flat.

In conclusion, this study shows that: (a) It may be possible to model the dynamics of large root systems as the sum of many short, absorbing roots. (b) It may be possible to measure K_r with steady-state measurements of *F* versus *P*. Best results will be achieved if the roots are perfused at 0.4 MPa pressure with distilled water and all measurements of *F* are made with

$P > 0.2$ MPa; the values might still be underestimated by 5 to 20%, however. The underestimate might be more if perfusion does not lower C_i much or if the solute permeability of the root is substantially less than that of maize roots. (c) It may be possible to measure K_r with high accuracy if measurements of *F* versus *P* can be performed during a period of <50 s. Although it is possible to make a flowmeter with a response time < 1 s (we have one now), it is not clear whether flow transients due to root elasticity or due to the compression of air bubbles (if present) in roots might prevent accurate measurements of *F* versus *P* in experiments lasting < 50 s.

APPENDIX

```
Program AMAIZED;
{WRITTEN IN TURBO PASCAL, BORLAND INTERNATIONAL}
uses dos, crt;
var
  i, j, k, m, mn, loop : integer;
  f1, f2: text;
  ch: char;
  a, b, cc, k1, k2, k3, k4, k5,{constants as defined below}
  Jw, tcy, {water flux m3/s into base of root}
  dt, t, tp, tpc, dtp, dtpc, tn, {time interval, cum. time, print times}
  pa, po {pressures in sine function}: real;
  dC, C, {change in concn, concentration mole/m3}
  P, {pressure MPa}
  v {sap velocity in xylem vessel, m/s}: array[0..300] of real;
const
  n = 100; {number of finite elements used in simulation}
  L = 0.1; {root length m}
  dx = L/n; {finite element length, axial, m}
  diam = 0.001; {root diameter, m}
  LP = 2e − 7; {root radial conductivity m/(s MPa)}
  Lx = 5* Lp* 3.1415* diam* L* L; {axial conductance m3/s per
    MPa/m}
  D = 2e − 9; {salt diffusion coefficient, m2/s}
  Vf = 0.03; {volume fraction of root that is vessels = csa fraction}
  Js = 1.76e − 7; {salt uptake flux rate, mol/(m2 s)}
  Ps = 3e − 9; {salt radial permeability m/s}
  sRT = 0.7* 8.314* 293* 1e − 6; {reflection coef * R * T in MPa
    m3/mol}
  pi = 3.141592654;
  Co = 5; {outside concentration}
  csa = pi* diam* diam* Vf/4; {cross section of vessels}
Procedure GetSSPressure;
  {computes steady-state pressure gradient by successive
    approximation}
begin
  v[n]: = k1*(P[n] − sRT*(C[n] − Co)); {compute sap velocity}
  for i: = 1 to n − 1 do v[n − i]: = v[n + 1− i] + k1*(P[n − i] −
    sRT*(C[n − i] − Co));
  for i: = 1 to n do P[i]: = P[i-1] − v[i]* k5;
end;
begin
  clrscr;
  Writeln('Dynamic Gradient Osmotic Flow Model for Maize
    Root');
  Writeln('  by Mel Tyree');
  Writeln('Computation with P(t) = Po + Pa*sin(2pi(t/tcy)
    + 3pi/2)');
  Writeln;
  Write('Enter period for 2pi cycles of P[0], tcy: ');
  readln(tcy);
```

```
dt: = tcy/(50*24); if dt > 1 then dt: = 1;
Write('Enter pressure amplitude, Pa: '); readln(Pa);
Write('Enter average pressure, Po: '); readln(Po);
P[0]: = Po − Pa;
k1: = 4* dx* Lp/(diam* Vf);
k2: = 4* dt/(diam* Vf);
k3: = D* dt/dx;
k4: = dt/dx;
k5: = dx* csa/Lx; {absolute resistance per axial xylem section}
a: = Lp* sRT;
b: = Ps − Lp*(0 + sRT* Co);
cc: = −Js − Ps* Co; {start out at 0 P}
C[0]: = (−b + sqrt(b*b − 4*a*cc))/(2*a);
Writeln('Ci in stele of root: ',C[0]:7:4,' osmol/m3');
for i: = 0 to n do begin
    C[i]: = C[0]; {start with steady-state concn at root pressure =
        0 MPa}
    P[i]: = P[0];
end;
for j: = 1 to 10 do GetSSPressure;
dtp: = tcy/24;
tp: = dtp - 0.00001; {time intervals for data saves}
t: = 0;
assign(f1,'rootsd.dat');
rewrite(f1);
Writeln(' Flow m3/s P, MPa Time, s Velocity m/s');
loop: = 0;
  Repeat
    GetSSPressure;
    v[0]: = v[1];
    if v[n]>0 then dC[n]: = k2*(Js − Ps*(C[n] − Co))
        +k4*v[n − 1]*C[n − 1] + k3*(C[n − 1] − C[n])
      else dC[n]: = k2*(Js − Ps*(C[n] − Co)) + k4* v[n]*C[n] +
        k3*(C[n − 1] − C[n]);
    for i: = 1 to n − 1 do begin
        dC[i]: = k2*(Js − Ps*(C[i] − Co)) + k3*(C[i− 1] + C[i + 1]
            − 2* C[i]);
        if v[i]>0 then dC[i]: = dC[i] − k4*v[i]* C[i]
          else dC[i]: = dC[i] + k4*v[i]* C[i];
        if v[i − 1] >0 then dC[i]: = dC[i] + k4* v[i − 1]* C[i − 1];
        if v[i + 1] <0 then dC[i]: = dC[i] − k4* v[i + 1]* C[i + 1];
    end;
    for i:= 1 to n do C[i]: = C[i] + dC[i];
    t: = t + dt;
    P[0]: = Po + pa* sin(2* pi* t/tcy + 3* pi/2);
    if t > = tp then begin
        Jw: = v[1]* csa;
        Writeln(Jw:13,' ',P[0]:7:5,' ',t:8:3,' ',v[1]:12);
        Writeln(f1,Jw:13,' ',P[0]:7:5,' ',t:8:3);
        loop: = loop + 1;
        tp: = tp + dtp;
    end;
  Until loop = 49;{49 loops prints out slightly beyond two
        periods}
close(f1);
Writeln('Output filename: ROOTSD.DAT');
end.
```

LITERATURE CITED

Anderson WP, Aikman DP, Meiri A (1970) Excised root exudation—a standing gradient osmotic flow. Proc R Soc Lond Biol Sci 174: 445–458

Azaizeh H, Steudle E-D (1991) Effects of salinity on water transport of excised maize (Zea mays L.) roots. Plant Physiol 97: 1136–1145

Bréda N, Cochard H, Dreyer E, Granier A (1993) Water transfer in a mature oak stand (Quercus petraea): seasonal evolution and effects of drought. Can J For Res 23: 1136–1143

Cermák J, Huzulak J, Penka M (1980) Water potential and sap flow rate in adult trees with moist and dry soil as used for the assessment of root system depth. Biol Plant 22: 34–41

Christy AL, Ferrier JM (1973) A mathematical treatment of Münch's pressure-flow hypothesis of phloem translocation. Plant Physiol 52: 531–538

Fiscus EL, Kramer PJ (1975) General model for osmotic and pressure-induced flow in plant roots. Proc Natl Acad Sci USA 72: 3114–3118

Frensch J, Steudle E (1989) Axial and radial hydraulic resistance to roots of maize (Zea mays L.) Plant Physiol 91: 719–726

Goeschl JD, Magnuson CE, DeMichele DW, Sharpe PJH (1976) Concentration-dependent unloading as a necessary assumption for a closed form mathematical model of osmotically driven pressure flow in phloem. Plant Physiol 58: 556–562

Nobel PS (1991) Physicochemical and Environmental Plant Physiology. Academic Press, New York

Nobel PS, Sanderson J (1984) Rectifier-like activities of roots of two desert succulents. J Exp Bot 35: 727–737

North GB, Ewers FW, Nobel PS (1992) Main root—lateral root junctions of two desert succulents: changes in axial and radial components of hydraulic conductivity during drying. Am J Bot 79: 1039–1050

Peterson CA, Murrmann M, Steudle E-D (1993) Location of the major barriers to water and ion movement in young roots of Zea mays L. Planta 190: 127–136

Tyree MT, Christy AL, Ferrier JM (1974) A simpler iterative steady-state solution of Münch pressure-flow systems applied to long and short translocation paths. Plant Physiol 54: 589–600

Tyree MT, Cochard H, Cruiziat P, Sinclair B, Ameglio T (1993a) Drought-induced leaf shedding in walnut: evidence for vulnerability segmentation. Plant Cell Environ 16: 879–882

Tyree MT, Ewers FW (1991) The hydraulic architecture of trees and other woody plants. New Phytol 119: 345–360

Tyree MT, Sinclair B, Lu P, Granier A (1993b) Whole shoot hydraulic resistance in Quercus species measured with a new high-pressure flowmeter. Ann Sci For 50: (in press)

Valancogne C, Nasr Z (1989a) Measuring sap flow in the stem of small trees by a heat balance method. Hortscience 24: 383–385

Valancogne C, Nasr Z (1989b) Une méthode de mesure du débit de séve brute de petits arbres par bilan de chaleur. Agronomie 9: 609–617